



Chinese Pedigree of Chronic Mucocutaneous Candidiasis Due to *STAT1* Gain-of-Function Mutation: A Case Study and Literature Review

Xu Wang · Weiwei Zhao · Feng Chen · Peiru Zhou · Zhimin Yan

Received: 11 June 2022 / Accepted: 18 October 2022 / Published online: 6 November 2022
© The Author(s), under exclusive licence to Springer Nature B.V. 2022

Abstract

Objective To further elucidate the clinical, immunological and genetic features of chronic mucocutaneous candidiasis (CMC) due to *STAT1* GOF mutation in the Chinese population.

Methods Clinical data for a proband were collected, and pedigree analyses were performed. Whole-exome sequencing and targeted Sanger sequencing were conducted to explore genetic factors of a Chinese pedigree involving inherited CMC.

Results An autosomal dominant CMC pedigree was identified, and both the proband and his father had mucocutaneous *Candida* infections without involvement of other systems. A rare mutation (c.T1175C) in *STAT1* was detected in this CMC pedigree. Multiple sequence alignment revealed that the amino acid position of this mutation (p.M392T) is evolutionarily conserved in vertebrate species. Serum IFN- α was elevated in patients harbouring the mutation. A total of 10 publications reporting 26 CMC patients with *STAT1* GOF mutations were retrieved by literature review, and the most common mutation found in previously reported Chinese patients is T385M in the DNA-binding domain.

Conclusions *STAT1* GOF mutation at c.T1175C (p.M392T) may lead to mucocutaneous *Candida* infections and an increase in serum IFN- α . T385M in the DNA-binding domain is the most common *STAT1* GOF mutation found in the Chinese population.

Handling Editor: Xiao Meng.

Supplementary Information The online version contains supplementary material available at <https://doi.org/10.1007/s11046-022-00685-y>.

X. Wang · W. Zhao · P. Zhou (✉) · Z. Yan (✉)
Department of Oral Medicine, Peking University School and Hospital of Stomatology & National Center of Stomatology & National Clinical Research Center for Oral Diseases & National Engineering Research Center of Oral Biomaterials and Digital Medical Devices, 22 ZhongguancunNandajie, Haidian District, Beijing 100081, People's Republic of China
e-mail: zhoupeiru1989@163.com

Z. Yan
e-mail: yzhimin96@163.com

F. Chen
Central Laboratory, Peking University School and Hospital of Stomatology, Beijing 100081, People's Republic of China

Keywords Chronic mucocutaneous candidiasis (CMC) · Signal transducer and activator of transcription 1 (STAT1) · Gain-of-function (GOF) mutation · Chinese

Introduction

Chronic mucocutaneous candidiasis (CMC) is a heterogeneous group of syndromes with the common feature of recurrent or persistent *Candida* infections of skin, nails and mucous membranes [1]. Inherited CMC is often caused by inborn errors of immunity, impairing the response to, or the production of IL-17A and IL-17F [2]. Mutations in signal transducer and activator of transcription 1 (*STAT1*), autoimmune regulator (*AIRE*), caspase recruitment domain family member 9 (*CARD-9*) and *Dectin-1* (also known as C-type lectin domain family 7 member A, *CLEC7A*) are the main factors contributing to inherited CMC [3]. Among them, *STAT1* gain-of-function (GOF) mutations have been demonstrated to be the most common cause of inherited CMC, and account for more than half of cases [4].

The Janus kinases (JAKs)-STAT signalling pathway plays a critical role in transducing signals from various cytokines to achieve distinct transcriptional outcomes. STAT1 is a critical transcription factor that mediates cell signalling in response to type I, II, and III interferons (IFNs) and interleukin (IL)-27 [4]. JAKs become activated when IFNs and IL-27 bind to JAKs' two chains, and activated JAKs lead to phosphorylation of STAT1. Phosphorylated STAT1 forms homodimers, heterodimers or multimers, and translocates to the nucleus, where it regulates transcriptional programmes [4, 5]. There are different phenotypes caused by *STAT1* mutation, including autosomal recessive (AR) complete loss-of-function (LOF), AR partial LOF, autosomal dominant (AD) LOF, and AD GOF [5]. Among them, AD GOF *STAT1* mutations, which are characterized by hyperphosphorylation and delayed dephosphorylation of STAT1 in response to stimulation of cytokines, leading to Th17-cell deficiency by preventing Th17 polarization, are the main hereditary factor for CMC [6, 7]. More than 100 *STAT1* GOF mutation sites have been found globally [4]. The coiled-coil domain (CCD) and DNA-binding domain (DBD) account for the majority of these GOF mutation sites.

The immunological and clinical features of patients with *STAT1* GOF mutations show broad heterogeneity. A previous study reported that reduced CD4⁺ T cells, CD8⁺ T cells, CD19⁺ B cells, CD19⁺CD27⁺ memory B cells, and CD16⁺CD56⁺ NK cells can be found in 28%, 16%, 19%, 49%, and 25% of patients

with *STAT1* GOF mutations, respectively [8]. Regarding clinical manifestations, most patients with *STAT1* GOF mutations (approximately 98%) have CMC. Bacterial infection and viral infection are observed in 74% and 38% of patients, respectively [8]. In addition, autoimmune manifestations, such as hypothyroidism, type 1 diabetes mellitus, vitiligo and systemic lupus erythematosus (SLE) occur in more than one-third of patients [8]. Other manifestations, such as squamous cell carcinomas and aneurysms, have also been reported in some cases.

Since *STAT1* mutations were identified in patients with AD CMC in 2011 [9], the relationship between *STAT1* mutations and CMC has increasingly been explored [10]. However, the heterogeneity of the clinical, immunological and genetic features of these patients has not been elaborated entirely and should be further explored. In this study, we systematically examined a Chinese CMC pedigree and performed a literature review to further elucidate clinical, immunological and genetic features of CMC due to *STAT1* GOF mutation in the Chinese population.

Case Presentation

The proband (D1) was a 13-year-old boy who had an eight-year history of persistent white patches on the tongue and inner cheek. He was thin, but had no history of medical systemic disease. On physical examination, whitish plaques that could not be scraped off were seen on the tongue, lip and buccal mucosa, with a nodular nature on palpation. The bilateral angle of the lips was involved, manifesting chronic dry desquamation with redness. The skin of the hand joints also presented desquamation on multiangle lesions (Fig. 1A). Fungal culture of the saliva revealed oral *Candida albicans* infection. Biopsy of the dorsal tongue showed nondysplastic chronic hyperplastic epithelium with hyphal infiltration by periodic acid-Schiff (PAS) staining, indicating a pathological diagnosis of chronic hyperplastic candidiasis.

Analysis of all leukocyte subsets showed an increased monocyte count ($1.01 \times 10^9/L$) and ratio (13.5%). In addition, a slightly reduced ratio of CD4⁺ helper T cells to CD8⁺ suppressor T cells (0.85) was found by a blood test, though the populations of CD4⁺ T cells and CD8⁺ T cells were normal. Immunological examination showed highly elevated serum

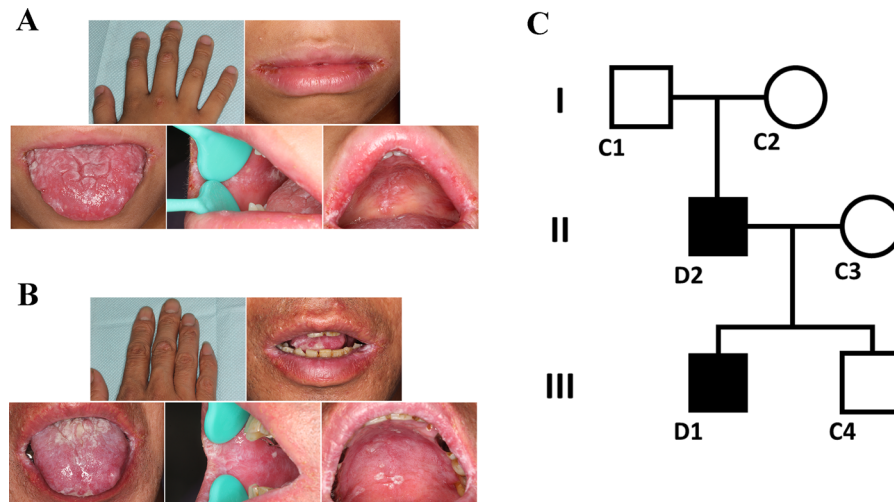


Fig. 1 Clinical characteristics of the proband and his family. Clinical images of the proband (**A**) and his father (**B**). Whitish plaques surrounded with erythematous and inflamed lesions could be seen on the tongue, buccal and palate; chronic dry desquamation with redness could be seen on the bilateral

angular of the lips; desquamation on multiangle lesions could be seen on the skin of the hand joints. **C** Family pedigree. An autosomal dominant heterozygous mutation was detected in the proband (D1) and his father (D2)

concentrations of IgG (17.1 g/L) and slightly elevated anti-nuclear antibody titre (1:40) (Table 1). Further antinuclear antibody spectrum tests (including anti-ENA, anti-nRNP, anti-SSA, anti-SSB, anti-Scl-70, anti-PM-Scl, anti-ribosomal P, anti-histones, anti-Sm, anti-JO-1, anti-PCNA, anti-CENP B, anti-AMA-M2, anti-Ro-52, anti-ds-NDA, and anti-nucleosome) and laboratory examinations of thyroid function showed no abnormalities (Table S1 and Table 1).

There was also a family history. His father (D2) had experienced similar oral and skin symptoms for a long time, which had not been taken seriously (Fig. 1B). Conversely, the proband's grandparents, mother, and brother did not have persistent or recurrent oral or cutaneous candidiasis. Given the proband's clinical manifestations, laboratory examinations, and family history (Fig. 1C), familial CMC caused by inherited gene mutations was suspected.

Methods

Genetic Analysis

Whole-exome sequencing (WES) was performed using genomic DNA samples from all family members in three generations. Briefly, genomic DNA extracted from peripheral blood was fragmented to an average

size of 180–280 bp and subjected to DNA library construction using established Illumina paired-end protocols. The Illumina NovaSeq 6000 platform (Illumina Inc., San Diego, CA, USA) was utilized for genomic DNA sequencing by Novogene Bioinformatics Technology Co., Ltd (Beijing, China). After sequencing and filtering, clean reads were aligned to the reference human genome (hs37d5) using the Burrows-Wheeler Aligner (bwa) [11], and duplicate reads were marked using sambamba tools [12]. Single-nucleotide variants (SNVs) and indels were called with samtools to generate gVCF [13]. Copy number variants (CNVs) were detected with CoNIFER software (V0.2.2) [14]. Annotation was performed using ANNOVAR [15]. Filtering of rare variants was carried out, and potentially deleterious variations were reserved. In addition, the American College of Medical Genetics and Genomics (ACMG) was employed to better predict the harmfulness of variation. Candidate genes were screened from deleterious variants, dominant/recessive inheritance, and genotype/phenotype relationships. Finally, the causative mutation found by WES was validated by Sanger sequencing.

Table 1 Laboratory examination of blood

Test items	Results	Unit	Reference intervals
White blood cell count	9.3	10 ⁹ /L	3.5–9.5
Neutrophil count	4.14	10 ⁹ /L	1.8–6.3
Lymphocyte count	1.90	10 ⁹ /L	1.1–3.2
Monocyte count	1.01	↑ 10 ⁹ /L	0.1–0.6
Eosinophil count	0.37	10 ⁹ /L	0.02–0.52
Basophils count	0.04	10 ⁹ /L	0–0.06
Neutrophil %	65.9	%	40–75
Lymphocyte %	20.5	%	20–50
Monocyte %	13.5	↑ %	3–10
Eosinophil %	4.9	%	0.4–8
Basophils %	0.6	%	0–1
Total T lymphocytes CD3%	73.0	%	55.0–82.0
Total B lymphocytes CD19%	11.2	%	9.0–29.0
Suppressor/cytotoxic T cell CD8%	33.3	%	14.0–34.0
Helper T cell CD4%	28.3	%	25.0–57.0
CD4/CD8 ratio	0.85	↓	1.1–2.0
Natural killer cell CD16/56%	11.0	%	7.0–40.0
IgG level	17.1	↑ g/L	5.66–14.25
IgM level	0.96	g/L	0.3–2.09
IgA level	2.61	g/L	0.8–5
C3	1.54	g/L	0.91–1.57
C4	0.36	g/L	0.14–0.44
Parathormone	35.3	pg/mL	15–65
Thyrotropin receptor antibody	< 0.80	IU/L	0–1.75
TOTT3	2.41	nmol/L	1.34–2.73
TOTT4	121.55	nmol/L	78.38–157.4
FT3	5.62	pmol/L	3.28–6.47
FT4	13.28	pmol/L	7.9–18.4
TSH	1.78	μ IU/MI	0.56–5.91
Anti-nuclear antibodies	1:40		Negative
Anti-dsDNA antibodies	Negative		Negative

Multiple Sequence Alignment and Protein Structure Prediction

The human (*Homo sapiens*), zebrafish (*Danio rerio*), chicken (*Gallus gallus*), mouse (*Mus musculus*), pig (*Sus scrofa*), and rat (*Rattus norvegicus*) STAT1 protein sequences in fasta format were retrieved from UniProt (<https://www.uniprot.org/>). For multiple sequence alignment, T-coffee (<https://www.ebi.ac.uk/Tools/msa/tcoffee/>), a multiple sequence alignment server, was used to compare sequences. A graphical representation of the multiple sequence alignment was obtained from WebLogo ([http://weblogo.](http://weblogo.threeplusone.com/)

[threeplusone.com/](http://weblogo.threeplusone.com/)), a sequence logo generator [16]. For protein structure prediction, the sequences of wild-type and mutant *STAT1* detected in our study were uploaded to SWISS-MODEL (<https://swissmodel.expasy.org/>), an online homology modelling server [17], to obtain the three-dimensional (3D) structure models. In addition, the residue report for mutation in the STAT1 protein (Met392Thr in protein P42224) was obtained from the VarSite database (<https://www.ebi.ac.uk/thornton-srv/databases/cgi-bin/VarSite/GetPage.pl?home=TRUE>).

Serum Cytokine Quantification and Comparison

To investigate the influence of *STAT1* mutation on peripheral immunity, serum cytokine concentrations were quantified using an ABplex Human Cytokine 12-Plex Assay Kit (RK04296, ABclonal Technology Co., Ltd., Wuhan, China) by ABclonal Technology Co., Ltd. (Wuhan, China) according to the manufacturer's protocols. Briefly, 50 μ L of standards and serum were added to 96-well plates, and 5 μ L of coded microspheres were added and incubated for 1 h at 37 °C. After washing, 50 μ L of detection antibody was added to each well and incubated for 0.5 h at 37 °C. Next, 50 μ L of streptavidin- P-phycoerythrin (SA-PE) was added and incubated for 15 min at 37 °C in the dark. After washing with wash buffer, the fluorescence code and intensity were detected by ABplex-100 to draw a standard curve and calculate the concentration of each cytokine.

The six family members were divided into two groups, with D1 and D2 being assigned to the mutation group and the others (C1–C4) to the wild-type group. There were only two samples in the mutation group, and comparisons between groups were based on raw data.

Literature Review

A literature search was conducted on February 12, 2022. Five databases were searched: PubMed, Web of Science, EMBASE, Scopus, and CNKI (a Chinese database). The key search terms used were as follows: Keywords CONTAINS “*STAT1*” or “Signal Transducer and Activator of Transcription 1,” or Title CONTAINS “*STAT1*” or “Signal Transducer and Activator of Transcription 1” AND Keywords CONTAINS “CMC” or “Chronic mucocutaneous candidiasis” or “candidiasis” or Title CONTAINS “CMC” or “Chronic mucocutaneous candidiasis” or “candidiasis” AND Keywords CONTAINS “Chinese” or “China” or “CN” or Title CONTAINS “Chinese” or “China” or “CN” or the affiliation belongs to China. Suitable articles were identified by screening the abstract and full text, and duplicate articles or cases were excluded. All Chinese cases with CMC due to *STAT1* GOF mutation available online between January 2011 and January 2022 in articles, reviews, editorials, letters, and correspondence, written in English or Chinese, were included.

Results

Detection of an Inherited *STAT1* GOF Mutation Set

WES was carried out to identify sequence variation among the family members. An inherited mutation in *STAT1* was detected (Fig. 2A and Fig. 2B), c.T1175C (p.M392T) in the DNA-binding domain (DBD) (Fig. 2C), and validated in D1 and D2 according to Sanger sequencing (Fig. 2D). Referring to a previous study enrolling 274 patients with *STAT1* mutation from 40 countries [8], the mutation found in our study is a *STAT1* GOF mutation.

Evolutionary Conservation Test and 3D Structure Prediction of the Mutant *STAT1* Protein

To predict the importance of the amino acid at this position, a multiple sequence alignment was examined, revealing that M392 is evolutionarily conserved in vertebrate species (Fig. 3A and Fig. 3B). This suggests that genetic variants at this position are likely deleterious, in keeping with the ACMG results. Furthermore, a residue report from VarSite summarized that the methionine (Met) residue at position 392 is very highly conserved and is very likely to be important for the protein's function; thus, variation at this position is unfavourable in terms of conserved amino acid properties. In addition, Met at position 392 is hydrophobic and has an aliphatic side chain. Conversely, the variant residue, threonine (Thr), has a neutral side chain, which may influence the structure of the protein. The predicted 3D structures of the wild-type and mutant *STAT1* proteins were obtained from SWISS-MODEL (Fig. 3C).

Profiling of Peripheral Blood Cytokines

A panel of 12 human cytokines was used to investigate the influence of *STAT1* mutation on peripheral immunity in this family. We captured some trends from the results. The IFN- α level was increased in the *STAT1* mutation group compared with the wild-type group (45.03 ± 5.22 pg/ml vs. 37.10 ± 0.36 pg/ml), though IL-17A (3.21 ± 0.07 pg/ml vs. 3.21 ± 0.04 pg/ml) and IFN- γ (7.60 ± 0.30 pg/ml vs. 7.44 ± 0.31 pg/ml) levels were not significantly altered (Fig. 4). No significant difference in IL-1 β , IL-

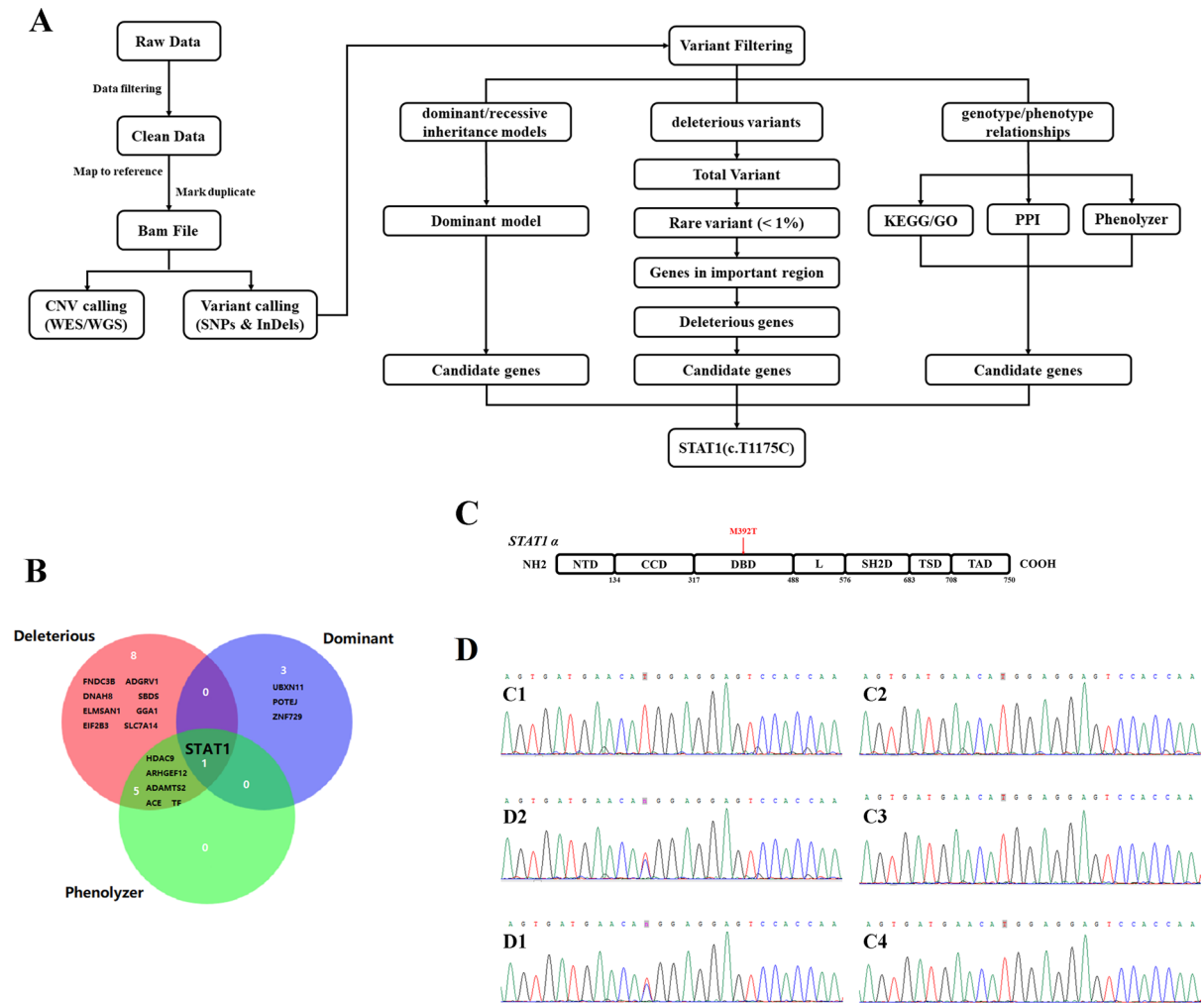


Fig. 2 *STAT1* was screened as the causative gene. **A** Pathogenic variant screening process of whole-exome sequencing and analysis. *STAT1* (c.T1175C) was found to be the causative mutation. **B** A Venn diagram of candidate genes screened from deleterious variants, dominant/recessive inheritance, and genotype/phenotype relationships. **C** The position of the p.M392T mutation in the human *STAT1* α isoform, NTD = N-terminal

domain, CCD = coiled-coil domain, DBD = DNA-binding domain, L = linker domain, SH2D = SH2 domain, TSD = tail segment domain, TAD = transactivation domain. **D** Sanger sequencing validation of the potential causative mutation in this family, the mutation (c.T1175C) in D1 and D2 was heterozygous

2, IL-4, IL-5, IL-6, IL-8, IL-10, IL-12P70 and TNF- α levels was found between the mutation group and wild-type group (Figure S1).

Characteristics of Chinese CMC Patients with *STAT1* GOF Mutation

Through the literature search, a total of 10 publications reporting 26 CMC patients with *STAT1* GOF mutations were identified (Table S2). The most common mutation found in these Chinese patients was T385M

in the DNA-binding domain (Fig. 5A). The median age of patients who began to have candidiasis was 1 year (1 month–5 years); the median age of patients diagnosed with *STAT1* GOF mutations was 10 years and 8 months (14 months–30 years) (Table S2). Approximately two thirds of the patients were male (Table S2). Oral candidiasis was found in 100% of the patients (Fig. 5B). In addition, 13 of these patients had pneumonia and/or bronchopneumonia, and thyroid disease was found in 7 patients (Fig. 5C).

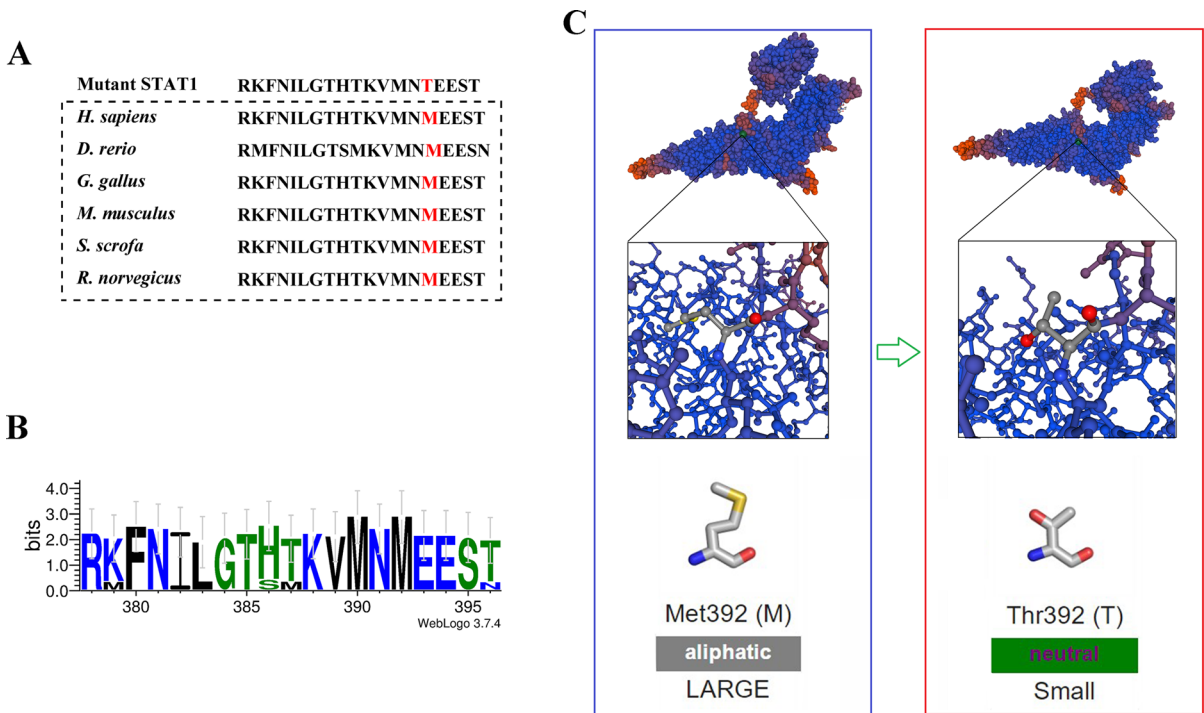


Fig. 3 Prediction of the potential deleterious effects of *STAT1*, c.T1175C (p.M392T). **A** Multiple sequence alignment. Met392 in *STAT1* was evolutionary conserved. **B** Graphical representation of the multiple sequence alignment (dotted box of

Fig. 3A). **C** Protein structure analysis. Methionine (Met) at position 392 is hydrophobic; the variant residue threonine (Thr) is neutral

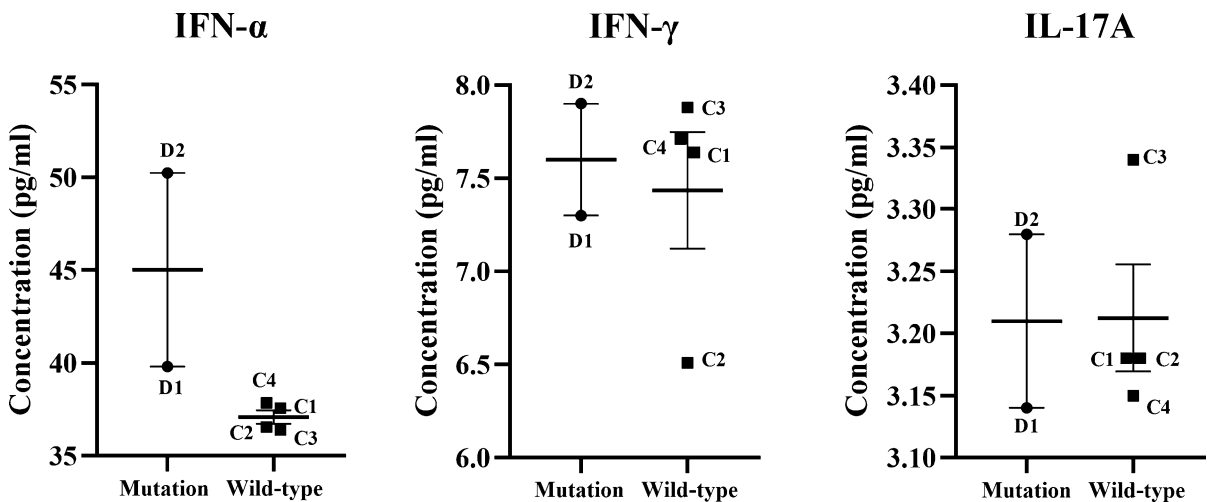


Fig. 4 Serum levels of IFN- α , IFN- γ and IL-17A in *STAT1* GOF mutation patients (mutation group) and their families (wild-type group). The results are shown as the mean \pm SEM

Discussion

STAT1 GOF mutation is considered to be the most common genetic factor of inherited CMC, and is

always associated with various infectious and autoimmune features. Approximately 112 missense/nonsense mutations in *STAT1* have been registered in the Human Gene Mutation Database (HGMD). It is quite

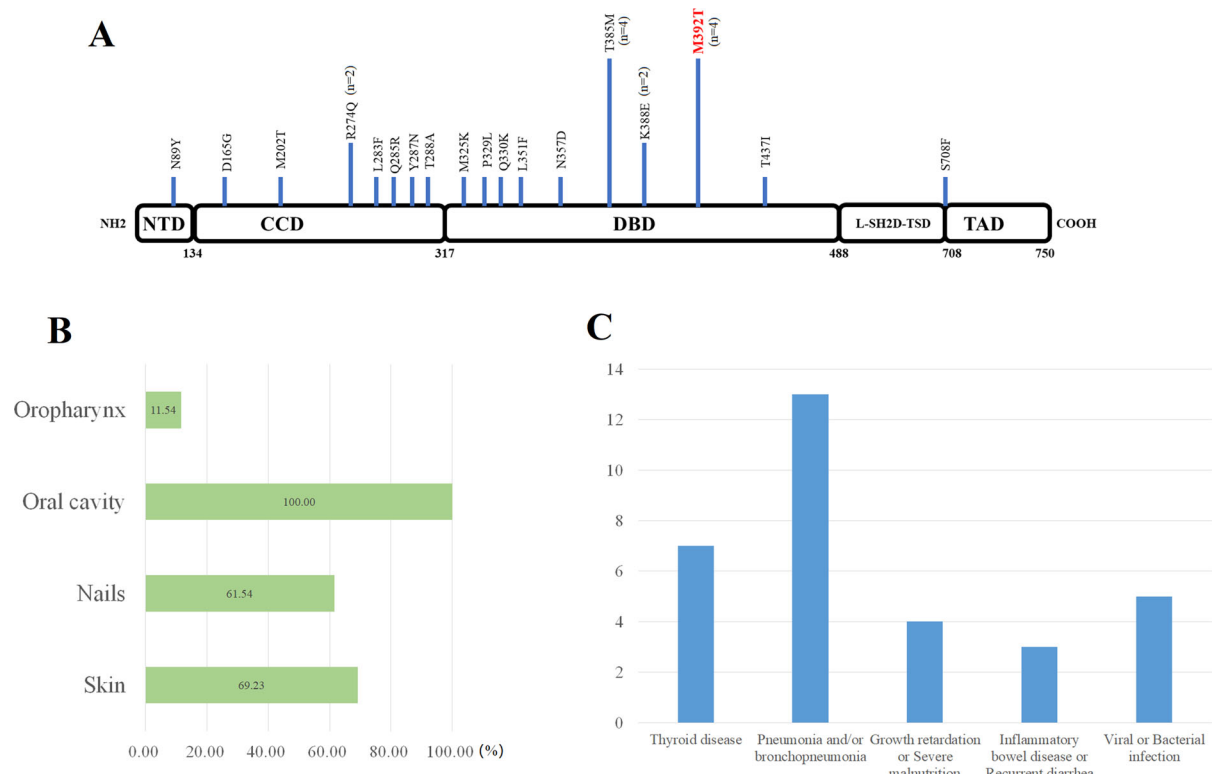


Fig. 5 Characteristics of CMC patients with *STAT1* GOF mutations reported in the Chinese population. **A** Locations of the reported mutations in the *STAT1* protein; the length of the blue line represents the number of cases reported with mutation

possible that the function of various mutation sites differs; thus, the clinical features in these patients are heterogeneous. In the present case, the clinical characteristics of the proband who developed CMC without systemic abnormalities were described in detail, and a Chinese pedigree with an inherited *STAT1* GOF mutation (c.T1175C) was identified. Evolutionary conservation analysis and 3D structure prediction of the mutant *STAT1* protein were performed to verify the functional mutation. Cytokine profiling in peripheral blood was performed to explore the immune state beyond immune cells, and revealed elevated IFN- α levels. By a literature review, some characteristics of Chinese CMC patients with *STAT1* GOF mutations were revealed.

The diagnosis of CMC associated with primary immune deficiencies is based on clinical history, including careful family history, identification of differentiating clinical and immunological features

at that location. **B** Percentage of fungal infection sites. **C** Other common manifestations found in Chinese CMC patients with *STAT1* GOF mutation; the vertical axis represents the number of cases

associated with particular molecular causes, and genetic analysis, especially *STAT1* GOF mutations [4].

Although there are various mutations in *STAT1*, A267V, R274Q and R274W in the coiled-coil domain seem to be most common [4, 18]. The M392T mutation found in our study is a relatively rare mutation and was first reported in a 23-year-old French male [8] in an article reviewing 274 patients with *STAT1* GOF mutations, but no details of this mutation were provided. Interestingly, a recent case report also described the clinical features of a Chinese pedigree with the *STAT1* M392T mutation [19]. A 30-year-old woman and her brother had mild CMC since early childhood, with the M392T mutation being the main cause. These clinical features are consistent with the proband of our study. Therefore, we deduce that this mutation may result in mild clinical symptoms, and CMC beginning in early childhood may be the main feature. Nevertheless, considering that it is an AD inheritance disease, prenatal testing is

recommended, especially when approximately 6% of patients with *STAT1* GOF mutations will probably develop squamous cell carcinoma [8]. Thus, close follow-up is also necessary for these patients.

The clinical characteristics of Chinese CMC patients due to *STAT1* GOF mutation have not been explored before. In this study, we reviewed 10 publications reporting 26 Chinese CMC patients with *STAT1* GOF mutations, and found that T385M was the most common. Oral candidiasis was the most common manifestation and was found in all patients. Moreover, autoimmune diseases such as thyroid disease, were found in 26.9% of the patients, which was similar to a previous study of 22% [8]. However, there was a delay between the median age of symptom onset (1 year) and definitive diagnosis (10 years and 8 months) in these patients, which indicated a missed diagnosis for many patients.

The mechanisms by which *STAT1* GOF contributes to CMC are complex and under exploration. The most accepted theory regarding susceptibility to CMC in patients with *STAT1* GOF mutation is failure to dephosphorylate nuclear pSTAT1 [20]. Hyperphosphorylation of STAT1 leads to a persistent response to IFNs and IL-27, which are inhibitors of Th17 cells [6]. IL-17 is considered to be the main effector molecule for the host to fight against fungal infection, the deficiency of which leads to susceptibility to fungi, such as *Candida* spp [21]. Low CD3⁺IL-17⁺ or CD4⁺IL-17⁺ T lymphocytes and reduced peripheral blood mononuclear cell (PBMC) IL-17 production (measured after 12 h of stimulation with *Candida*) have been reported in 82% and 40% of patients with *STAT1* GOF, respectively [8]. In our study, the number of CD4⁺ T lymphocytes and the concentration of serum IL-17A in the proband were normal. As more than 80% of *STAT1* GOF patients are reported to have a reduced frequency of Th17 cells in the peripheral blood, further verification should be carried out to determine whether the number of Th17 cells in the proband's peripheral blood and his IL-17 production function of the PBMCs under *Candida* stimulation are normal.

Autoimmune manifestations, such as hypothyroidism (approximately 22%) and skin disease (approximately 10%), are also common manifestations in patients with *STAT1* GOF mutation. The most accepted mechanism of this feature is also due to hyperphosphorylation of STAT1, which can

upregulate IFN-stimulated genes (ISGs) in response to IFNs and IL-27 [22]. The additional IFN signal may lead to autoimmunity, such as autoantibody formation. High IgG can be found in approximately 20% of patients with *STAT1* GOF mutation [8], playing important roles in autoimmune diseases, such as rheumatoid arthritis, SLE, and immunothrombocytopenia [23]. Although no abnormalities were found based on autoimmune antibody tests, the proband reported in this study is at risk of developing autoimmune disease in the future, as he was positive for anti-nuclear antibodies, and his serum IFN- α and IgG levels were elevated. The sample size we used for cytokine detection was limited, and the retrieved Chinese cases did not undergo cytokine testing, making it difficult to further comprehensively analyse the relationship between the clinical manifestations and cytokine levels. Therefore, further large-scale clinical trials are needed to draw conclusions.

Given the nature of the disease, an optimal management strategy is still lacking. Long-term antifungal treatment is necessary for most patients with *STAT1* GOF mutation [18]. Among them, fluconazole is always the main first-line oral therapy, followed by itraconazole or posaconazole. For patients with clinical resistance to antifungal agents, second- or third-line treatments (voriconazole, echinocandins, terbinafine or liposomal amphotericin B) are required [4]. For patients with primary immunodeficiencies, hematopoietic stem cell transplantation [24] can be a curable treatment and Janus kinase (JAK) inhibitors such as ruxolitinib [25, 26] might improve CMC and autoimmune manifestations in some cases.

In conclusion, we reported a Chinese pedigree with AD CMC caused by a *STAT1* GOF mutation at c.T1175C (p.M392T) in the DNA-binding domain. We confirmed that the detected mutant site is very highly conserved based on the evolutionary conservation analyses. The clinical manifestations of the proband were described in detail, and elevated serum IFN- α was detected in *STAT1* GOF mutation patients. From these results, it is speculated that the *STAT1* GOF mutation at c.T1175C (p.M392T) may lead to mucocutaneous *Candida* infections and an increase in serum IFN- α . Additionally, T385M in the DNA-binding domain is the most common *STAT1* GOF mutation found in the Chinese population.

Author Contributions X.W. performed experiments and wrote original draft. W.W.Z. collected sample. F.C. performed genetic analysis. P.R.Z. collected sample and clinical data. Z.M.Y. provided scientific guidance and supervised the study.

Funding This work was financially supported by the National Natural Science Foundation of China (Nos. 81570985 and 82170967) and Beijing Natural Science Foundation (No. 7204330).

Availability of Data and Material The raw data supporting the conclusions of this article are available on request to the corresponding authors.

Declarations

Conflict of interest The authors declare no conflicts of interest with respect to the authorship and/or publication of this article.

Consent to Participate Written informed consent was obtained from the individuals (D2, C1, C2, and C3) or the guardians (D1 and C4) for the publication of any potentially identifiable images or data included in this article.

Ethics Approval Study protocol was approved by the Biomedical Ethics Committee of Peking University School and Hospital of Stomatology (PKUSSIRB-201950163).

References

- Glocker E, Grimbacher B. Chronic mucocutaneous candidiasis and congenital susceptibility to *Candida*. *Curr Opin Allergy Clin Immunol*. 2010;10:542–50.
- Puel A. Human inborn errors of immunity underlying superficial or invasive candidiasis. *Hum Genet*. 2020;139:1011–22.
- Carey B, Lambourne J, Porter S, Hodgson T. Chronic mucocutaneous candidiasis due to gain-of-function mutation in STAT1. *Oral Dis*. 2019;25:684–92.
- Okada S, Asano T, Moriya K, Boisson-Dupuis S, Kobayashi M, Casanova JL, et al. Human STAT1 gain-of-function heterozygous mutations: chronic mucocutaneous candidiasis and type I interferonopathy. *J Clin Immunol*. 2020;40:1065–81.
- Olbrich P, Freeman AF. STAT1 and STAT3 mutations: Important lessons for clinical immunologists. *Expert Rev Clin Immunol*. 2018;14:1029–41.
- Zheng J, van de Veerdonk FL, Crossland KL, Smeekens SP, Chan CM, Al ST, et al. Gain-of-function STAT1 mutations impair STAT3 activity in patients with chronic mucocutaneous candidiasis (CMC). *Eur J Immunol*. 2015;45:2834–46.
- Liu L, Okada S, Kong XF, Kreins AY, Cypowyj S, Abhyankar A, et al. Gain-of-function human STAT1 mutations impair IL-17 immunity and underlie chronic mucocutaneous candidiasis. *J Exp Med*. 2011;208:1635–48.
- Toubiana J, Okada S, Hiller J, Oleastro M, Lagos GM, Aldave BJ, et al. Heterozygous STAT1 gain-of-function mutations underlie an unexpectedly broad clinical phenotype. *Blood*. 2016;127:3154–64.
- van de Veerdonk FL, Plantinga TS, Hoischen A, Smeekens SP, Joosten LA, Gilissen C, et al. STAT1 mutations in autosomal dominant chronic mucocutaneous candidiasis. *N Engl J Med*. 2011;365:54–61.
- Zhang W, Chen X, Gao G, Xing S, Zhou L, Tang X, et al. Clinical relevance of gain- and loss-of-function germline mutations in STAT1: a systematic review. *Front Immunol*. 2021;12: 654406.
- Li H, Durbin R. Fast and accurate short read alignment with Burrows–Wheeler transform. *Bioinformatics*. 2009;25:1754–60.
- Tarasov A, Vilella AJ, Cuppen E, Nijman IJ, Prins P. Sambamba: fast processing of NGS alignment formats. *Bioinformatics*. 2015;31:2032–4.
- Li H, Handsaker B, Wysoker A, Fennell T, Ruan J, Homer N, et al. The sequence alignment/map format and SAMtools. *Bioinformatics*. 2009;25:2078–9.
- Krumm N, Sudmant PH, Ko A, O’Roak BJ, Malig M, Coe BP, et al. Copy number variation detection and genotyping from exome sequence data. *Genome Res*. 2012;22:1525–32.
- Wang K, Li M, Hakonarson H. ANNOVAR: functional annotation of genetic variants from high-throughput sequencing data. *Nucleic Acids Res*. 2010;38: e164.
- Crooks GE, Hon G, Chandonia JM, Brenner SE. WebLogo: a sequence logo generator. *Genome Res*. 2004;14:1188–90.
- Arnold K, Bordoli L, Kopp J, Schwede T. The SWISS-MODEL workspace: a web-based environment for protein structure homology modelling. *Bioinformatics*. 2006;22:195–201.
- Depner M, Fuchs S, Raabe J, Frede N, Glocker C, Doffinger R, et al. The extended clinical phenotype of 26 patients with chronic mucocutaneous candidiasis due to gain-of-function mutations in STAT1. *J Clin Immunol*. 2016;36:73–84.
- Xu X, Meng W, Feng L, Guo W. New and inherited STAT1 mutations in a Chinese family with chronic mucocutaneous candidiasis: a case report. *Iran J Public Health*. 2020;49:1164–8.
- Fujiki R, Hijikata A, Shirai T, Okada S, Kobayashi M, Ohara O. Molecular mechanism and structural basis of gain-of-function of STAT1 caused by pathogenic R274Q mutation. *J Biol Chem*. 2017;292:6240–54.
- Kuwabara T, Ishikawa F, Kondo M, Kakiuchi T. The role of IL-17 and related cytokines in inflammatory autoimmune diseases. *Mediat Inflamm*. 2017;2017:3908061.
- Ostadi V, Sherkat R, Migaud M, Modarressadeghi SM, Casanova JL, Puel A, et al. Functional analysis of two STAT1 gain-of-function mutations in two Iranian families with autosomal dominant chronic mucocutaneous candidiasis. *Med Mycol*. 2021;59:180–8.
- Schwab I, Nimmerjahn F. Intravenous immunoglobulin therapy: How does IgG modulate the immune system? *Nat Rev Immunol*. 2013;13:176–89.
- Leiding JW, Okada S, Hagin D, Abinun M, Shcherbina A, Balashov DN, et al. Hematopoietic stem cell transplantation in patients with gain-of-function signal transducer and activator of transcription 1 mutations. *J Allergy Clin Immunol*. 2018;141(2):704–17

25. Bloomfield M, Kanderova V, Parackova Z, Vrabcova P, Svaton M, Fronkova E, et al. Utility of ruxolitinib in a child with chronic mucocutaneous candidiasis caused by a novel STAT1 gain-of-function mutation. *J Clin Immunol*. 2018;38(5):589–601.
26. Higgins E, Al Shehri T, McAleer MA, Conlon N, Feighery C, Lilib D, et al. Use of ruxolitinib to successfully treat chronic mucocutaneous candidiasis caused by gain-of-function signal transducer and activator of transcription 1 (STAT1) mutation. *J Allergy Clin Immunol*. 2015;135(2):551–3.

Springer Nature or its licensor (e.g. a society or other partner) holds exclusive rights to this article under a publishing agreement with the author(s) or other rightsholder(s); author self-archiving of the accepted manuscript version of this article is solely governed by the terms of such publishing agreement and applicable law.

Publisher's Note Springer Nature remains neutral with regard to jurisdictional claims in published maps and institutional affiliations.